Supporting Information
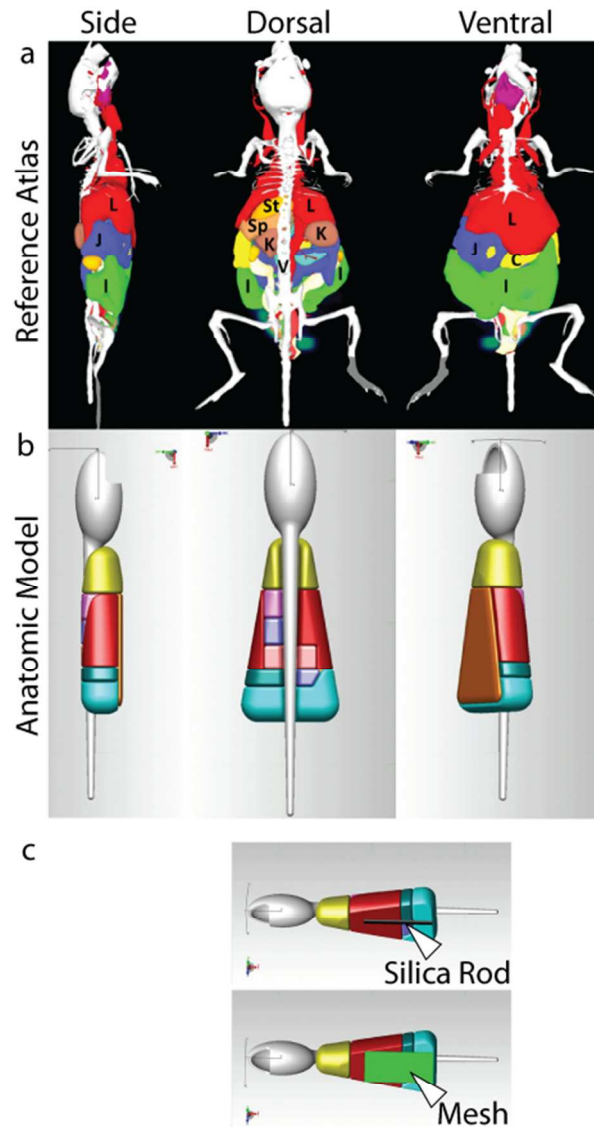
This supporting information includes:

Figure S1. Anatomic models of abdominal cavity used in fluence rate simulations. (a) Reference atlas overlay on tumor-bearing, female nude mouse from side, dorsal, and ventral orientations. (L, liver; J, jejunum (intestine); C, cecum (intestine); I, ileum (intestine); St, stomach; Sp, spleen; K, kidney; V, vertebral body) (b) Approximate anatomic model developed for simulations. Each tissue assigned optical coefficients for refraction, scattering, and absorption. (c) Models depicting implanted silica rod (top) and fiber optic mesh (bottom).
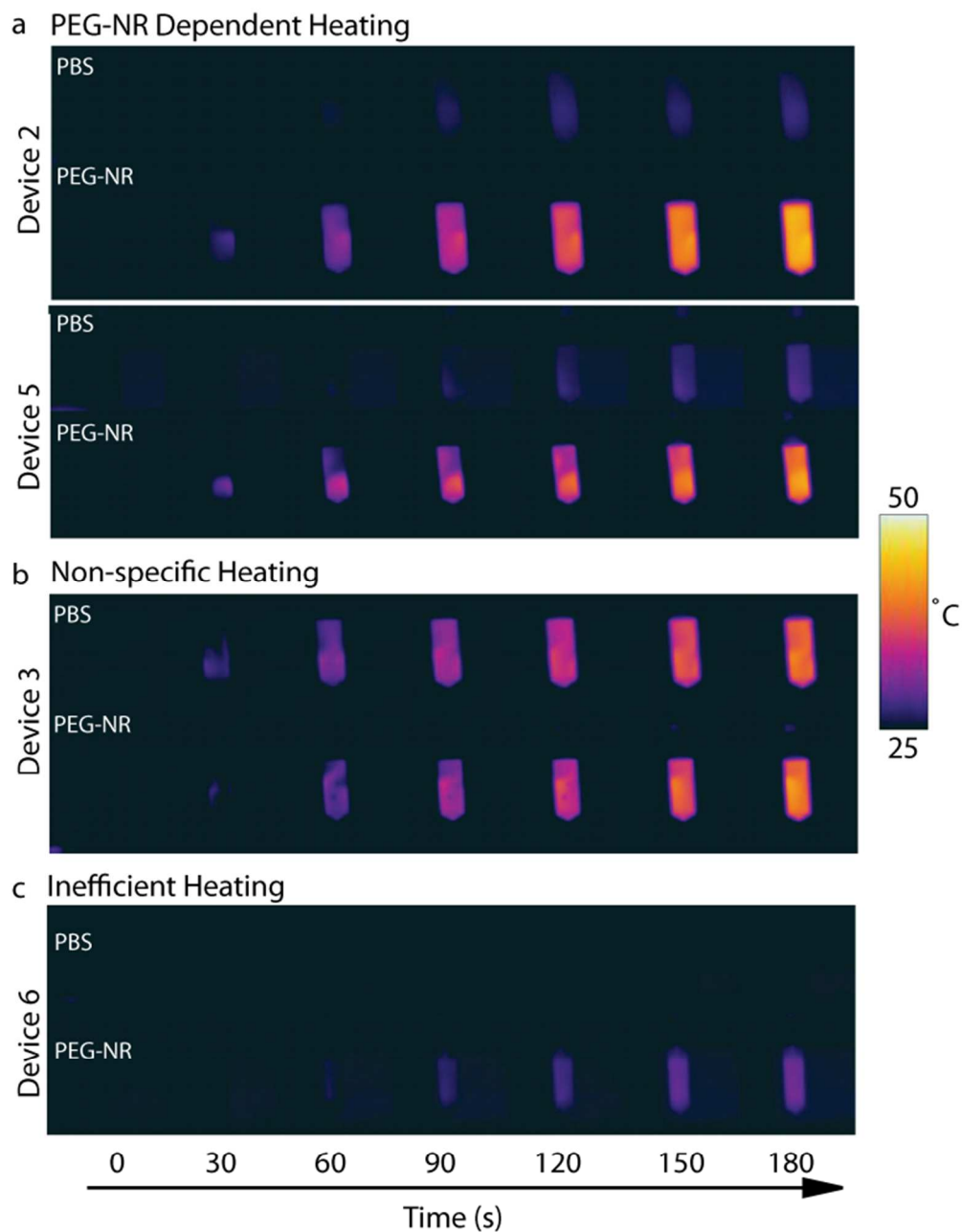
Figure S2. *Ex vivo* thermographic profiles for implantable devices. Images show devices 2, 3, 5, and 6 in solutions of PEG-NRs or control PBS. (a) Devices 2 and 5 demonstrate PEG-NR-dependent heating; (b) Device 3 demonstrates non-specific heating; (c) and Device 6 demonstrates inefficient heating.
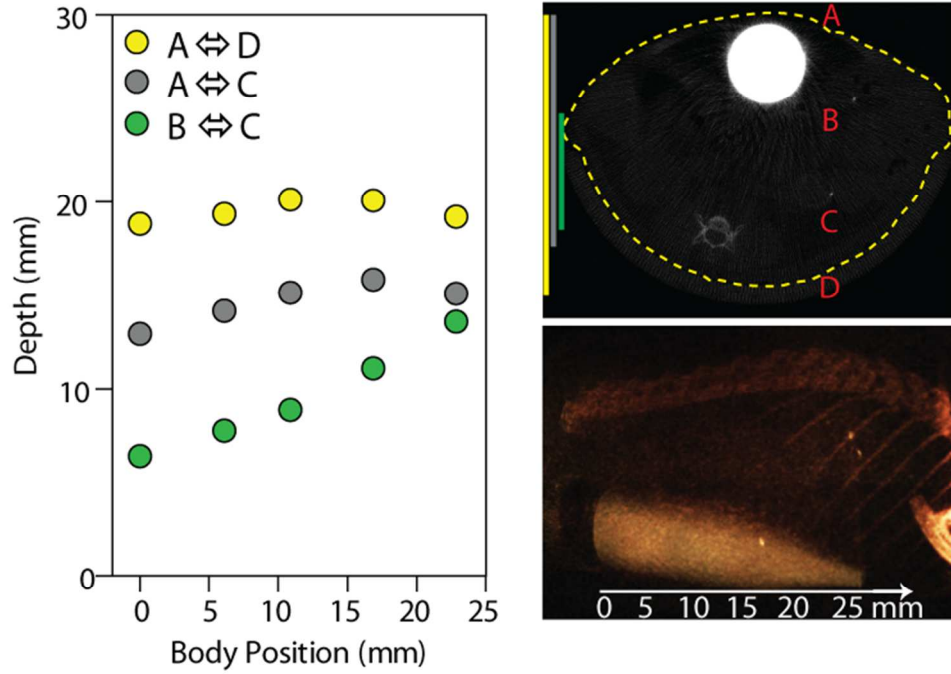
Figure S3. Measured distances between implanted device and anatomic landmarks. Landmarks include vertebrae, ventral and dorsal surfaces measured at multiple locations along body length by microCT image analysis.
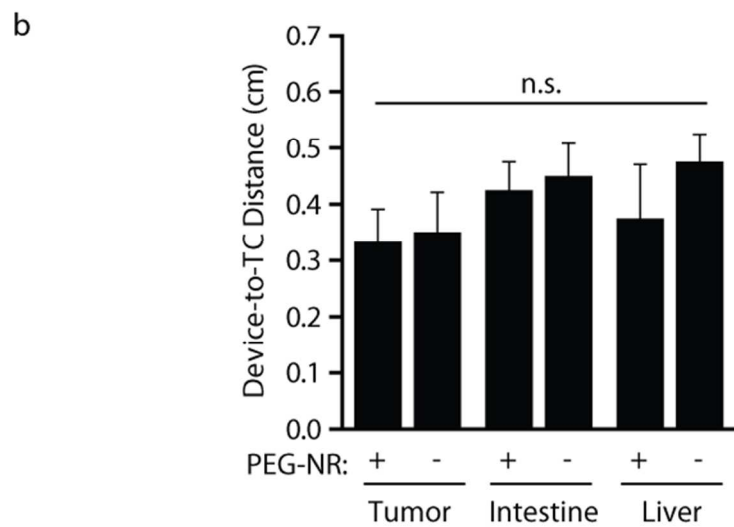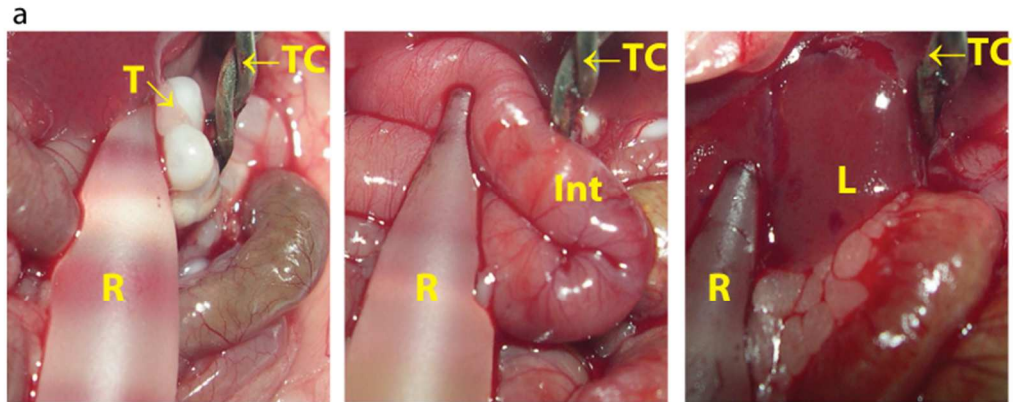
Figure S4. Measured distances between implanted device and thermocouple. (a) Representative images of implanted glass rod device (R), ovarian tumors (T), intestine (Int), liver (L), and thermocouple (TC). (b) Distances between implanted glass rod device and thermocouples for each tissue in presence or absence of PEG-NRs. (one-way ANOVA and Tukey's post test, *n*=4 for liver, intestine; *n*=2-3 for tumors). Error bars, s.d.

Tissue	Index of Refraction (808 nm)	Scattering Coefficient (cm^{-1})	Absorption Coefficient (cm^{-1})
Skin	1.550	200 [3]	1.3 [3]
Kidney	1.370	11 [1, 2]	0.01 [1, 2]
Lung	1.387	300 [3]	2.78 [3]
Liver	1.368	75 [5]	1.03 [5]
Stomach	1.383	47 [4]	0.19 [4]
Spleen	1.390	13 [1]	2.8 [1]
Intestine (Cecum)	1.380	10 [2]	0.02 [2]
Intestine (Jejunum)	1.380	10 [2]	0.02 [2]
Intestine (Ileum)	1.380	10 [2]	0.02 [2]

Table 1. Optical Coefficients for Modeling Simulations

1. Srinivasan, R.; Kumar, D.; Singh, M. Optical Tissue-Equivalent Phantoms for Medical Imaging. *Trends Biomater.* **2002**, *15*, 42-47.
2. Soloneno, M.; Cheung, R.; Busch, T.M.; Kachur, A.; Griffin, G.M.; Vulcan, T.; Zhu, T.C.; Wang, H.W.; Hahn, S.M.; Yodh, A.G. *In Vivo* Reflectance Measurements of Optical Properties, Blood Oxygenation, and Motexafin Lutetium Uptake in Canine Large Bowels, Kidneys, and Prostates. *Phys Med Biol* **2002**, *47*, 857-873.
3. Cheong, W.F.; Prahl, S.A.; Welch, A.J. A Review of the Optical Properties of Biological Tissues. *IEEE J. Quantum Electron.* **1990**, *26*, 2166-2185.
4. Bashkatov, A.N.; Genina, E.A.; Kochubey, V.I.; Gavrilova, A.A.; Kapralov, S.V.; Grishaev, V.A.; Tuchin, V.V. Optical Properties of Human Stomach Mucosa in the Spectral Range from 400 to 2000nm. *Med. Laser App.* **2007**, *22*, 95-104.
5. Ullah, H.; Atif, S.; Firdous, M.S.; Mehmood, M.; Ikram, C.; Kurachi, C.; Grecco, C.; Nicolodelli, G.; Bagnato, V.S. Femtosecond Light Distribution at Skin and Liver of Rats: Analysis for Use in Optical Diagnostics. *Laser Phys. Lett.* **2010**, *7*, 889-898.